Antenna Design to Extremes: Practicable Suggestions from Pattern Analysis and RICHWIRE Simulation of Special Delta-Cross Loops

N.I. Yannopoulou, P.E. Zimourtopoulos *

Antennas Research Group, Austria

Abstract

In order to investigate the ability of pattern analysis and RICHWIRE simulation we usually use, to further handle antenna designs under certain extreme geometric conditions, we set up a number of limiting cases of our Delta-Cross loop, an antenna shape which we devised for the additional purpose of this research. Specifically, we vary the wire radius, segment vicinity, apex angle, and central configuration, while we deliberately keep constant its total length at almost two wavelengths, and we demonstrate the results for its main antenna characteristics: the complex vector radiation pattern and the complex scalar input impedance, as well as, the real scalars directivity and SWR, respectively. In this way, we conclude practicable suggestions for managing antenna problems which particularly include similar geometric arrangements.

Keywords

Antenna, pattern, RICHWIRE, simulation, extreme, delta-cross

Introduction

The analytical study of the cross wire antenna of four λ/2 delta elements, as equilateral triangles with side length λ/6, was carried out with the available theoretical tools of a first semester university course. Thus, it was considered as a 5λ/4 two wired open circuit transmission line, bended appropriately to form the four delta elements with total length 2λ. The remaining two λ/4 segments formed a transmission line segment of opposite currents and so, they were not taking into account as they do not radiate at all [1]. The current was then taken as the standing wave current of the corresponding segment of a 2λ equivalent symmetric, centered fed, dipole antenna. The antenna is shown in Fig. 1.

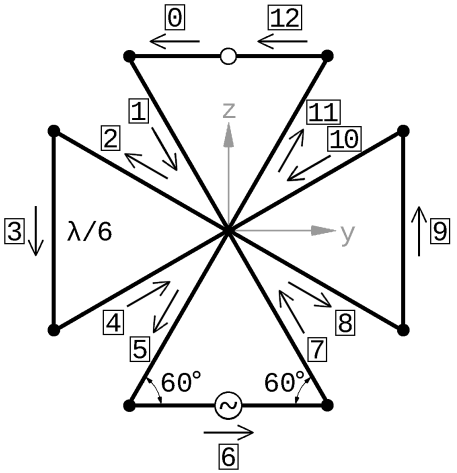

Fig. 1: The Planar Delta-Cross Shaped Loop antenna

The question is, was that approach adequately close to the current real situation, or accurately, near the simulated one and how can anyone verify it. From another point of view is the adopted theoretical model for the antenna geometry close enough to the simulated one which is undoubtedly closer to a possible built model. Some relative remarks are given in this paper. Additionally, the behavior of the antenna is presented, in detail, as the base angles of each delta loop varies between the two possible extremes values from 45° to 90°. The same tools will be used for the investigation, that is, the antenna theory for pattern analysis [2], the [RadPat4W] computer program of 2D/3D antenna patterns plots [3], the [RICHWIRE] simulation program [4] and the mini-Suite of software tools [5].

First Approach

The detailed procedure for the radiation pattern determination as a complex vector quantity had already be given in [1]. We repeat here the general relation that gives the total radiation pattern of all the 13 segments according to the law of superposition

$$\bar{\mathbb{E}} = \sum_{\nu=0}^{12} \begin{bmatrix} \dot{\mathbb{E}}_{\nu\theta} \\ \dot{\mathbb{E}}_{\nu\varphi} \end{bmatrix} = \begin{bmatrix} \dot{\mathbb{E}}_{\theta} \\ \dot{\mathbb{E}}_{\varphi} \end{bmatrix} = \dot{\mathbb{E}}_{\theta}\vec{\theta} + \dot{\mathbb{E}}_{\varphi}\vec{\varphi} = \quad (1)$$

$$= (\mathbb{E}_{\theta_R} + i\mathbb{E}_{\theta_I})\vec{\theta} + (\mathbb{E}_{\varphi_R} + i\mathbb{E}_{\varphi_I})\vec{\varphi}$$

which after a lot of manipulation and due to the antenna's symmetry was simplified as

$$\bar{\mathbb{E}} = \bar{\mathbb{E}}_{0,12,6} + \bar{\mathbb{E}}_{1,7} + \bar{\mathbb{E}}_{2,8} + \bar{\mathbb{E}}_{3,9} + \bar{\mathbb{E}}_{4,10} + \bar{\mathbb{E}}_{5,11} \quad (2)$$

were the real parts were eliminated. In [1], an upper bound of the absolute radiation pattern was illustrated. Actually it was the greatest possible upper bound since it resulted from the sum of the 13 absolute radiation patterns given by,

$$\left|\bar{\mathbb{E}}\right|_U = \sum_{\nu=0}^{12} \left|\bar{\mathbb{E}}_\nu\right| \quad (3)$$

while the absolute radiation pattern of the antenna is

$$\left|\bar{\mathbb{E}}\right| = \left|\sum_{\nu=0}^{12} \bar{\mathbb{E}}_\nu\right| = \left|\sum_{\nu=1}^{6} \bar{\mathbb{E}}_\mu\right| \quad (4)$$

where μ stands for each complex vector in (2). For the sake of research (5) gives another possible upper bound as the sum of the six absolute radiation patterns

$$\left|\bar{\mathbb{E}}\right|_u = \sum_{\mu=1}^{6} \left|\bar{\mathbb{E}}_\mu\right| \quad (5)$$

Fig. 2 shows the absolute radiation pattern of the antenna (4) among with its upper bounds of (3) and (5), all normalized to their maximum values in the three main planes, 1.27, 0.072 and 0.43, respectively for (3), (4) and (5). There is a noticeable difference, especially with the maximum upper bound given in [1]. The generalized triangle inequality dictates the relationship between them

$$\left|\bar{\mathbb{E}}\right| \le \left|\bar{\mathbb{E}}\right|_u \le \left|\bar{\mathbb{E}}\right|_U \quad (6)$$

as it is shown in Fig. 3, where all patterns are normalized with the max value of 1.27. Actually we have determine, in that way, the minimum and the maximum limit of the radiation pattern among which will be located every other pattern of any possible combination of the antenna elements.

The comparison between the analytical evaluated radiation pattern of the antenna and the one result in from simulation is given in Fig. 4(a). The significantly different shape of the radiation patterns lead us to investigate the simulated model.

The first thought is that a theoretical model assumes that instead of a wire antenna in space with current distribution on its surface, there is only a filament current distribution that follows the same shaped curve in space. Thus, we rerun the simulation program with variable wire radius from $1x10^{-3}$ [m], that was initially, to $1x10^{-9}$ [m], that is, reducing the wire radius as much as possible in order to achieve a filament "ExtraThin" wire, near to the theoretical prototype.

There are two factors that must taken into account:

i. The constraints imposed by the simulation program itself, relative to the used mathematical functions and

ii. The need of a quantity that will provide a criterion to stop reducing the radius.

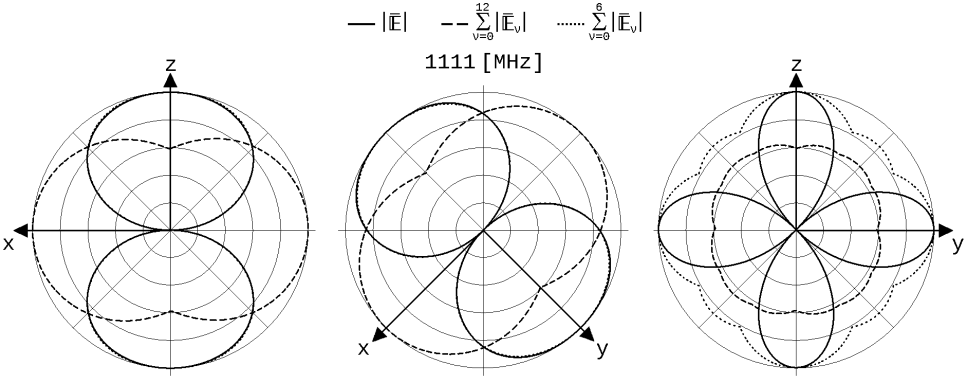

Fig. 2: Radiation patterns in 1111 [MHz]

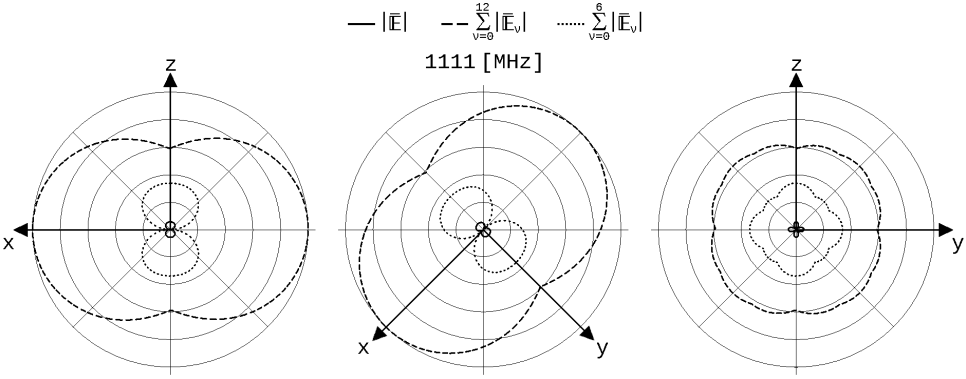

Fig. 3: Normalized patterns with common maximum value

The antenna Directivity is the right quantity to follow up since our concern is the radiation and it is shown in Fig. 5 with respect to the Wire Radius. The red line corresponds to the value 1 which is, as known, the directivity of an isotropic source, practically such an antenna does not exist, and it is the lower limit of Directivity. The two open circular points corresponds to the initial 1 [mm] radius (1.76) and to the radius of 0.5 [nm] (1.77) which represents the most thin wire that we may consider in the [RICH-WIRE] simulation program. In that radius Directivity has almost the same value as it shown with the straight black line in the figure. Beyond

that radius there is an unstable situation.

Fig. 4(b) illustrates all the patterns corresponding to the antenna with wire radius from $1x10^{-3}$ [m], to $1x10^{-9}$ [m]. The dotted black line is for the initial 1 [mm] and solid black line for the 0.5 [nm], which we named it as "ExtraThin". In Fig. (4c) the comparison between theory and simulation for the radiation pattern is shown, in the case of this ExtraThin wire.

Second Approach

The next idea is to find out if there is an explanation of the revealed difference between theory and simulation of the antenna radiation, shown in Fig. 4(a), relative to the analytical current assumption we considered.

As we already referred in [1] the simulation model was inevitable a little different from the theoretical one. Fig. 6 shows the three following steps:

(a) the initial theoretical model,

(b) the displacement of the four equilateral triangles by (2a+a/10)/2 away from their intersection point. Thus, a square is formed with side equal to 2a+a/10, where "a" is the used wire radius.

(c) the necessary connection of the neighboring sides of the delta elements by moving their apexes from the center of each side of the square to its corners.

A slight increase of the length of the base side of each delta element is necessary in order to reserve the 60° angle (60.006°) with its either sides. Therefore, the total length of each truncated triangle is by 2a+a/10 greater than the initial λ/2. Fig. 7 shows the small dashed square of Fig. 6, as a zoomed window.

This difference could result in a 1.55% to 4.67% change on the considered h quantity of the applied current distribution, if we take its ratio with respect to the total antenna length or to the length of the base of each delta element, respectively.

The significance of the base sides is due to the fact that the input source is located at the center of one of them. An investigation of the antenna radiation behavior in terms of h was carried out. It was varied in the range [4.5, 5.0] λ/4. Fig. 8 shows the horizontal maximum value of the normalized radiation pattern, i.e. on y axis for the selected arrangement. The noted point indicates the horizontal maximum value (0.51) of radiation pattern result in from [RICHWIRE].

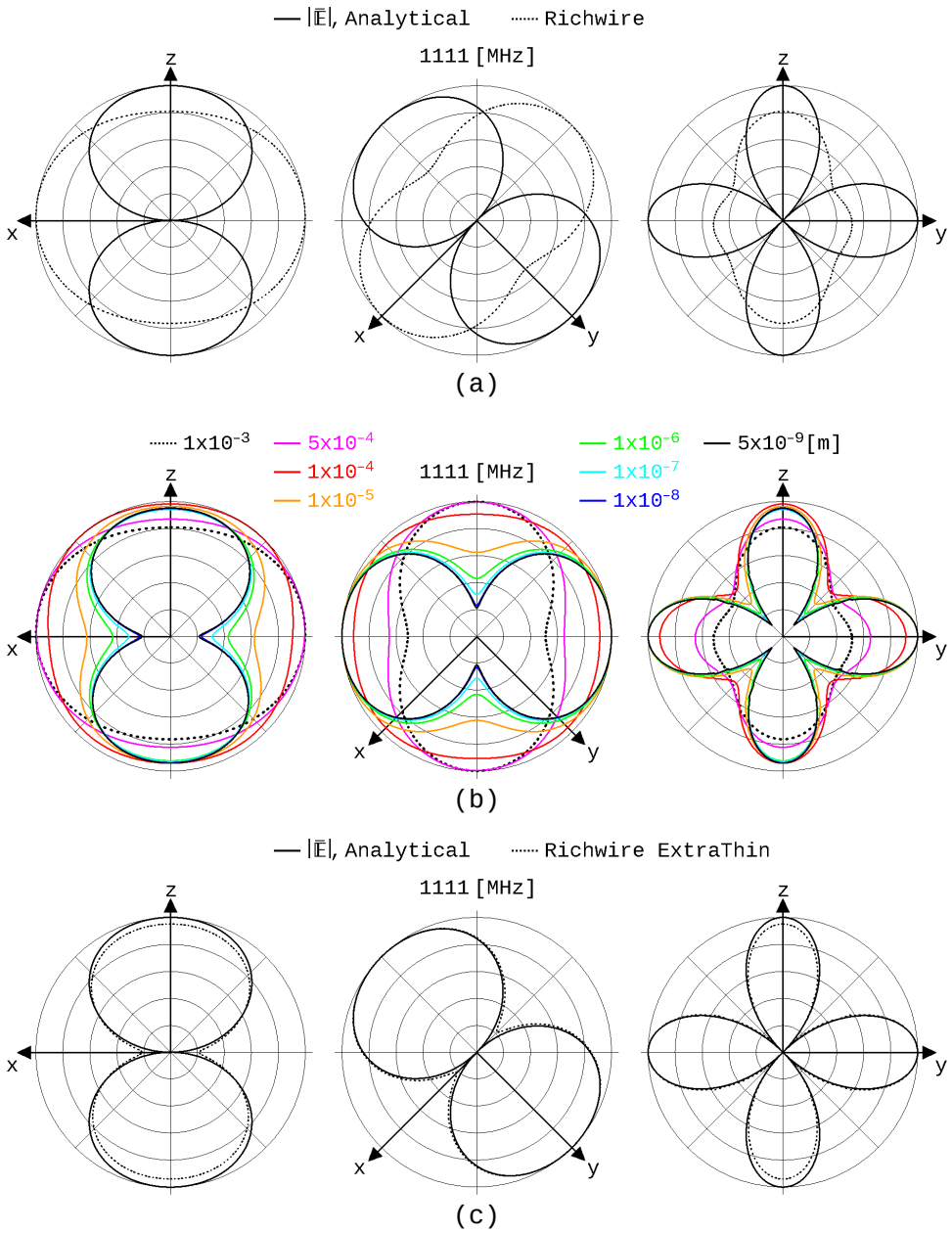

Fig. 4: Radiation pattern comparison

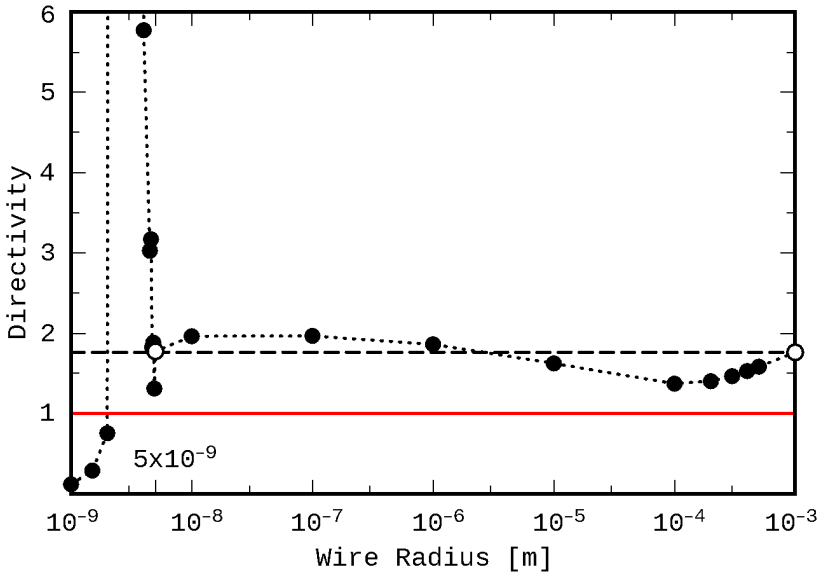

Fig. 5: Directivity versus Wire Radius

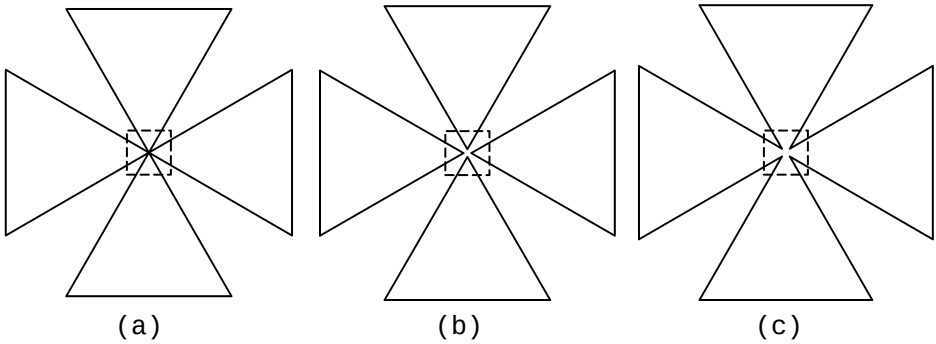

Fig. 6: Construction of the simulation model

This value corresponds to a h equal to 4.73λ/4, which is close enough to the 4.77 λ/4 as expected for the second percentage mentioned above ((100 – 4.67)% x 5.0 = 4.77). Since the other percentage leads to the value 4.92λ/4 of h, we decided to plot the radiation patterns in the three main planes for the range [4.5, 5.0] λ/4 of Fig. 9. From this figure is obvious that indeed the closest form

of the two patterns, theoretical and simulated, is achieved if we assume a sinusoidal current distribution with h equals to 4.73λ/4, as shown in Fig. 10.

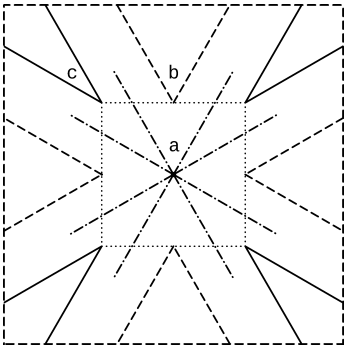

Fig. 7: Center detail

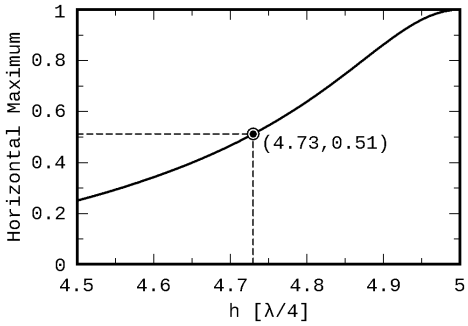

Fig. 8: Maximum value of radiation pattern on y axis

Modified Delta Element

The antenna was modified only with respect to the base angles of each delta element, keeping the perimeter constant, slightly greater than λ/2, as we already mentioned in the previous section, in order to improve its electric and electromagnetic characteristics [1], [7]. The result is a cross antenna of four isosceles triangles. We extent here the investigation to the whole possible range for the base angle, which is from 45° to 90°. Fig. 11 shows six representative geometries for 45°, 48°, 60°, 75°, 87° and 90° base angles. The base length of each antenna per wavelength is noted except in (f) where the side length is given instead.

The lower and upper limits lead to specific, degenerated cases, as it is shown in (a) and (f) of Fig. 11. In (a), a square is formed with the diagonal elements to be double as it is indicated by the small circular points near the center of the square. In fact, as the currents in those elements are of opposite direction it is expected that they do contribute almost nothing to the total radiation of such an antenna. At the upper limit, a cross is formed of double perpendicular elements. Since the distance between the λ/4 elements is too smaller than λ, and because their currents are again of opposite direction, no radiation is expected from them.

The remaining four small base elements of length (2a+ a/10), where "a" is the used

wire radius, i.e. 0.0021 [m], are small enough, as

$$\frac{0.0021}{\lambda} = 0.0078 < \frac{1}{10}\lambda \qquad (7)$$

and since the input source is on the one of the two parallel to y-axis elements while the other two parasitic elements are parallel to z-axis, λ/2 apart, we do expect a radiation like a small dipole on y-axis. These almost equivalent antennas are depicted in Fig. 12. Fig. 13 shows the comparison between the radiation patterns of the 45° Delta-Cross shaped loop antenna and of the equivalent simple Square loop one, with the same perimeter, on the three main planes, at 1111 [MHz].

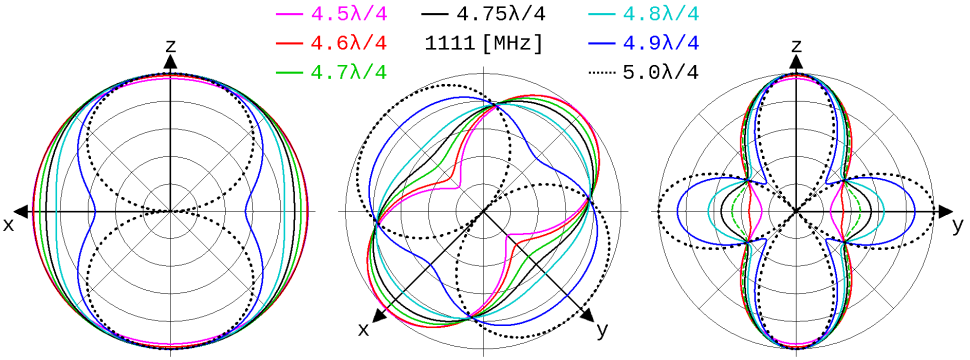

Fig. 9: Radiation patterns versus h

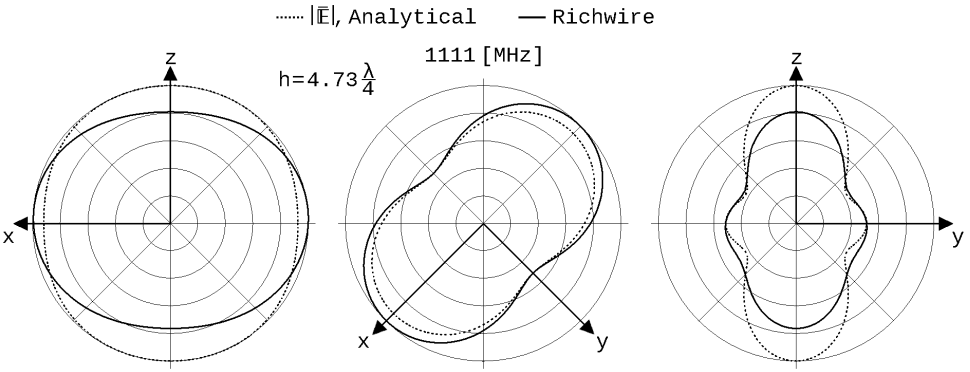

Fig. 10: Comparison of normalized patterns

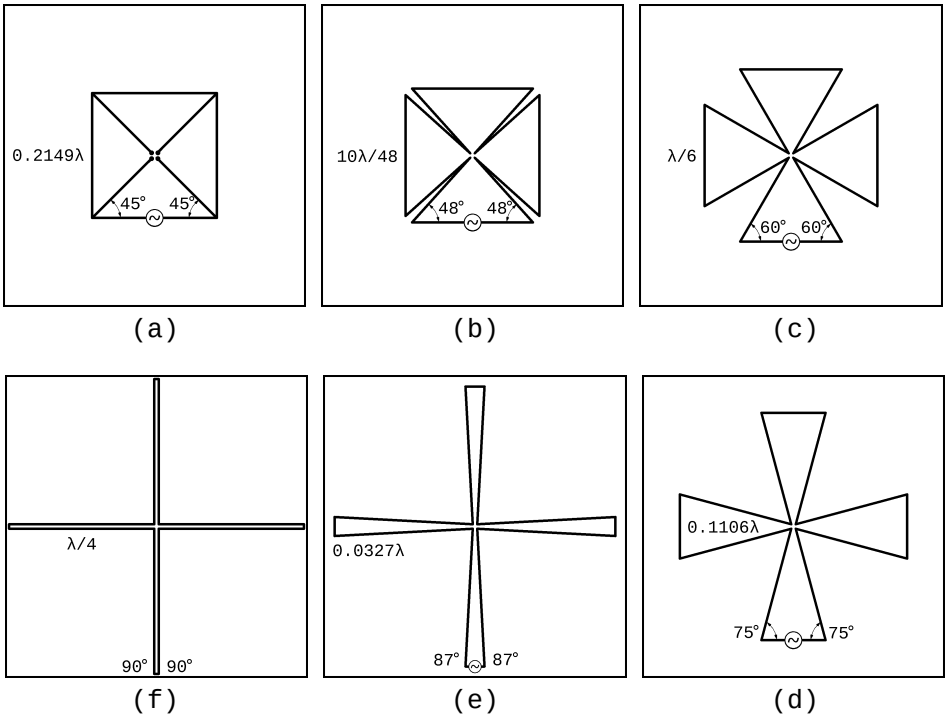

Fig. 11: Planar Delta-Cross shaped loop antennas

Fig. 14 contains the corresponding comparison between the 90° Delta-Cross shaped loop antenna, i.e. a rectangular shaped cross with λ/4 double sides, with a simple short dipole antenna parallel to y-axis. The agreement is obvious for both arrangements.

The investigation was performed in the range [45°, 90°] with 1° step at the frequencies 800, 1010 and 1111 [MHz], as these are the most interesting ones [1]. Fig. 15 shows the Directivity in [dB] with respect to the base angle. It is obvious that near the two limits of the degenerated cross antennas, the directivity shows a relative sharp change while at the frequency of 800 [MHz] has the more stable behavior. The two gray vertical lines correspond to 48° and 60° for the base angles of each delta element. The Directivity of the 48° Delta-Cross shaped loop antenna is greater at the higher frequencies.

SWR is given in Figs. 16, 17 and 18 for 50 [Ω], 75 [Ω] and 300 [Ω] respectively. The standing wave ratio is much better for the 48° not only for the 50 [Ω] but even for the 75 [Ω] characteristic impedance, at 1010 [Mhz].

Fig. 19 illustrates the Input Impedance [Z_{inp}] in terms of the base angle, in separate graphs for the Input Resistance [R_{inp}] and the Input Reactance [X_{inp}]. A narrower range for both the Resistance and the Reactance is given in Fig. 20, in order to clarify the behavior of the Input Impedance in lower values. It is obvious that the curve for 800 [MHz] is relative smooth both for the real and imaginary parts of the impedance while in the higher frequencies sharp changes appears as the base angle varies between 45° and 60°. In 1010 [MHz] a resonance is achieved for the 48° Delta-Cross antenna.

Conclusion

Two practical suggestions are given, in the present work, in order to explain the radiation pattern results from pattern analysis and simulation. The first is based on the assumption of the ExtraThin wire for simulation and the second to the inevitable change of the ideal geometrical representation in analysis to a more realizable model in simulation.

Both these different paths lead us to a good agreement between the, analytical and simulated, produced radiation patterns. Although, the simulation prototype could be closer to a constructed antenna and so the radiation pattern is expected to be as the result of simulation, the final step of the construction and measurement it is absolutely necessary to justify, as always, our expectations.

During this procedure the lower and the upper bound of the absolute radiation pattern for any possible deconstruction and reformation of the antenna in its elements was explicitly determined.

The detailed investigation on the range of the variable base angles reveals the two degenerated cases of 45° and 90° as the apex lower and upper bound, that is the design extremes, where the antenna is actually transformed to an equivalent common square loop and a short center fed dipole on y-axis respectively. It also becomes evident why the antenna of 48° base angle was selected as the improved Delta-Cross shaped loop antenna.

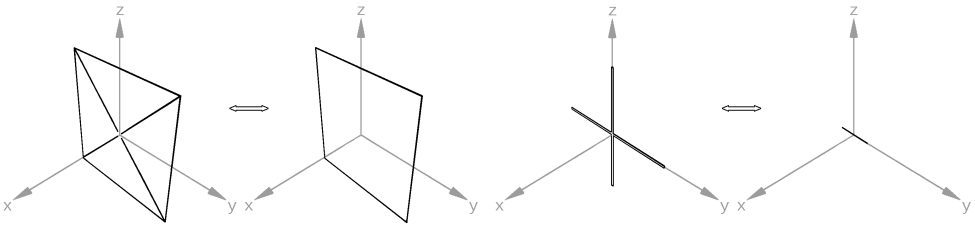

Fig. 12: Almost equivalent antennas in terms of radiation

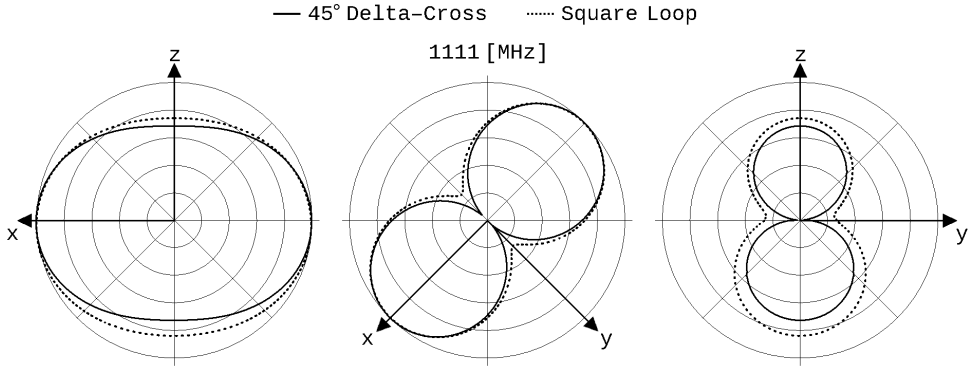

Fig. 13: 45° Delta-Cross and Square loop radiation

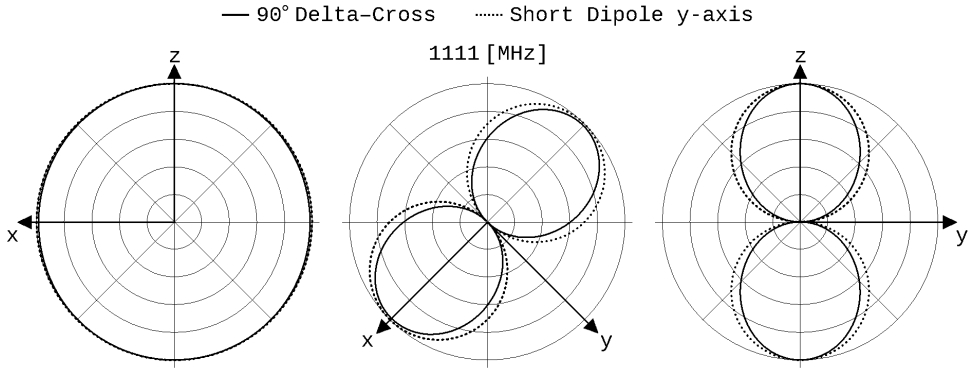

Fig. 14: 90° Delta-Cross and Short dipole on y-axis radiation

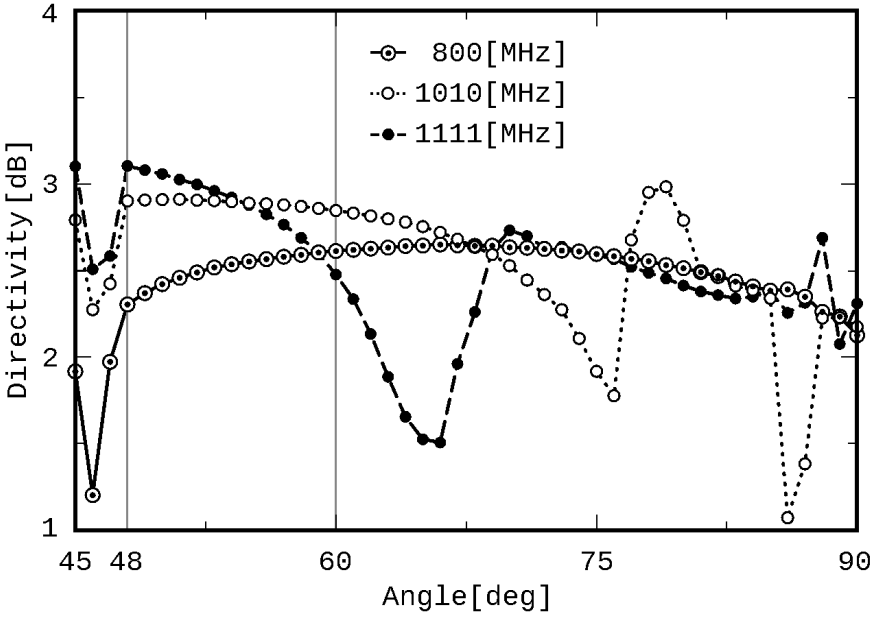

Fig. 15: Directivity versus base angle

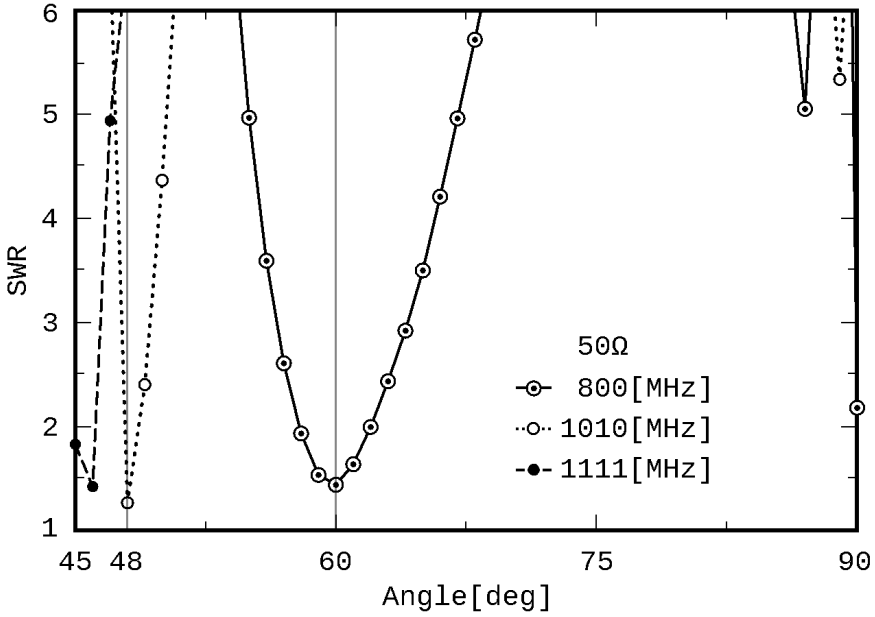

Fig. 16: SWR for 50 [Ω] characteristic impedance

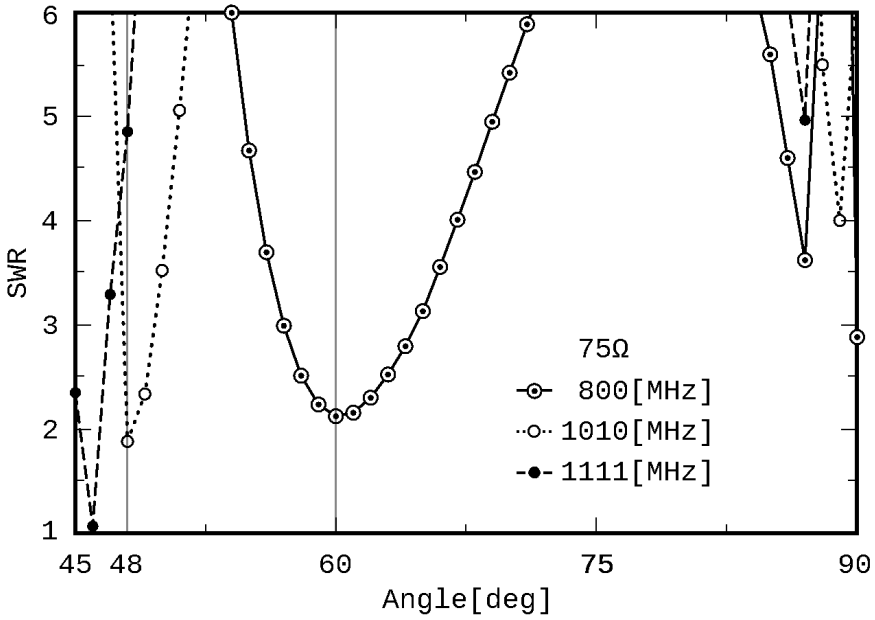

Fig. 17: SWR for 75 [Ω] characteristic impedance

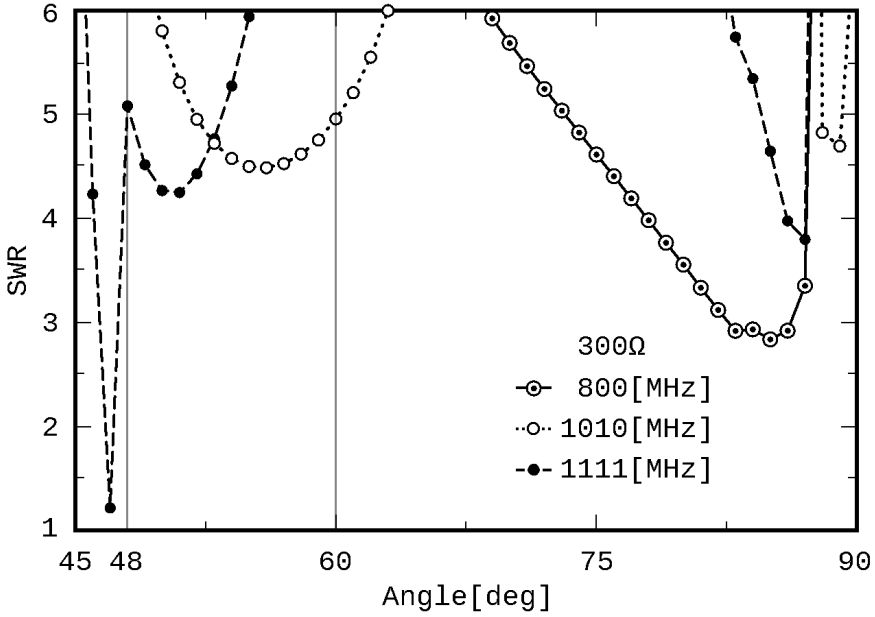

Fig. 18: SWR for 300 [Ω] characteristic impedance

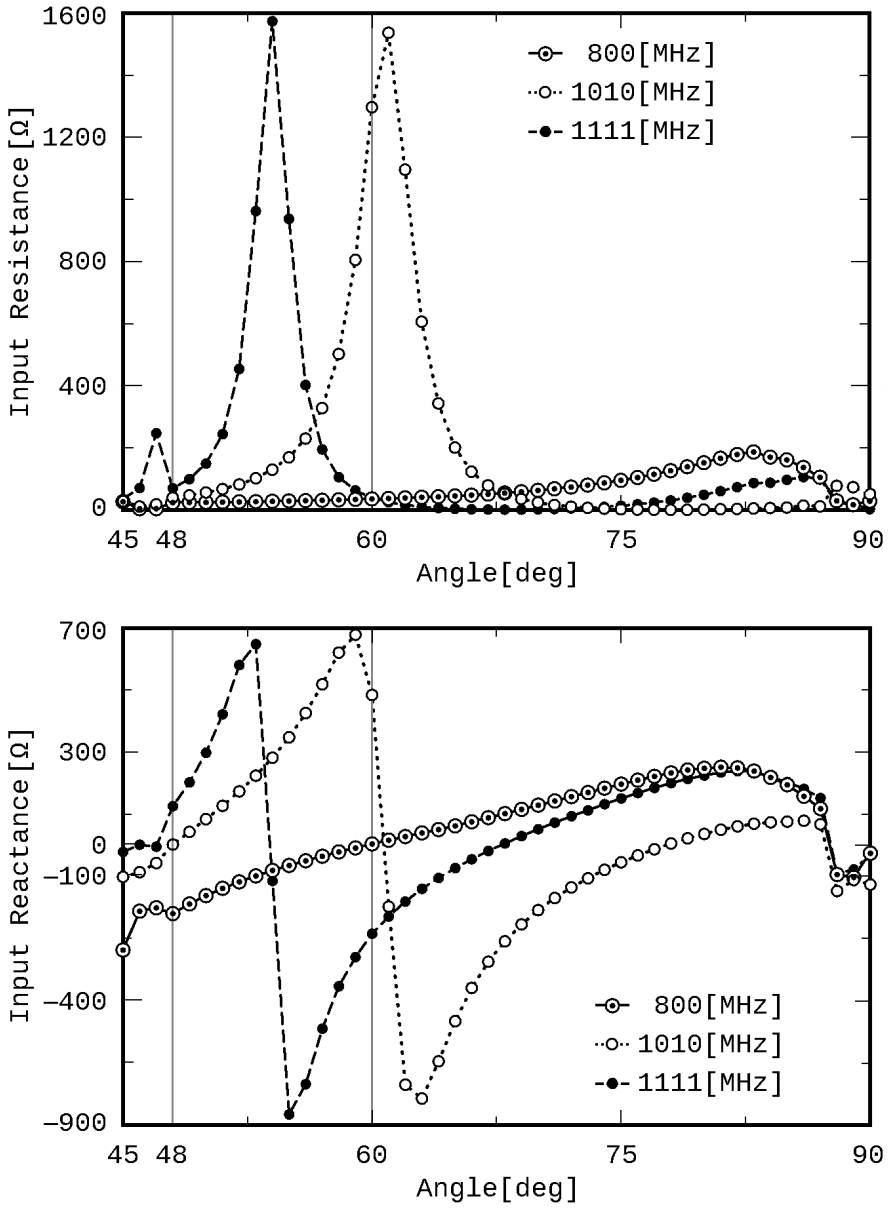

Fig 19: Input Impedance versus base angle

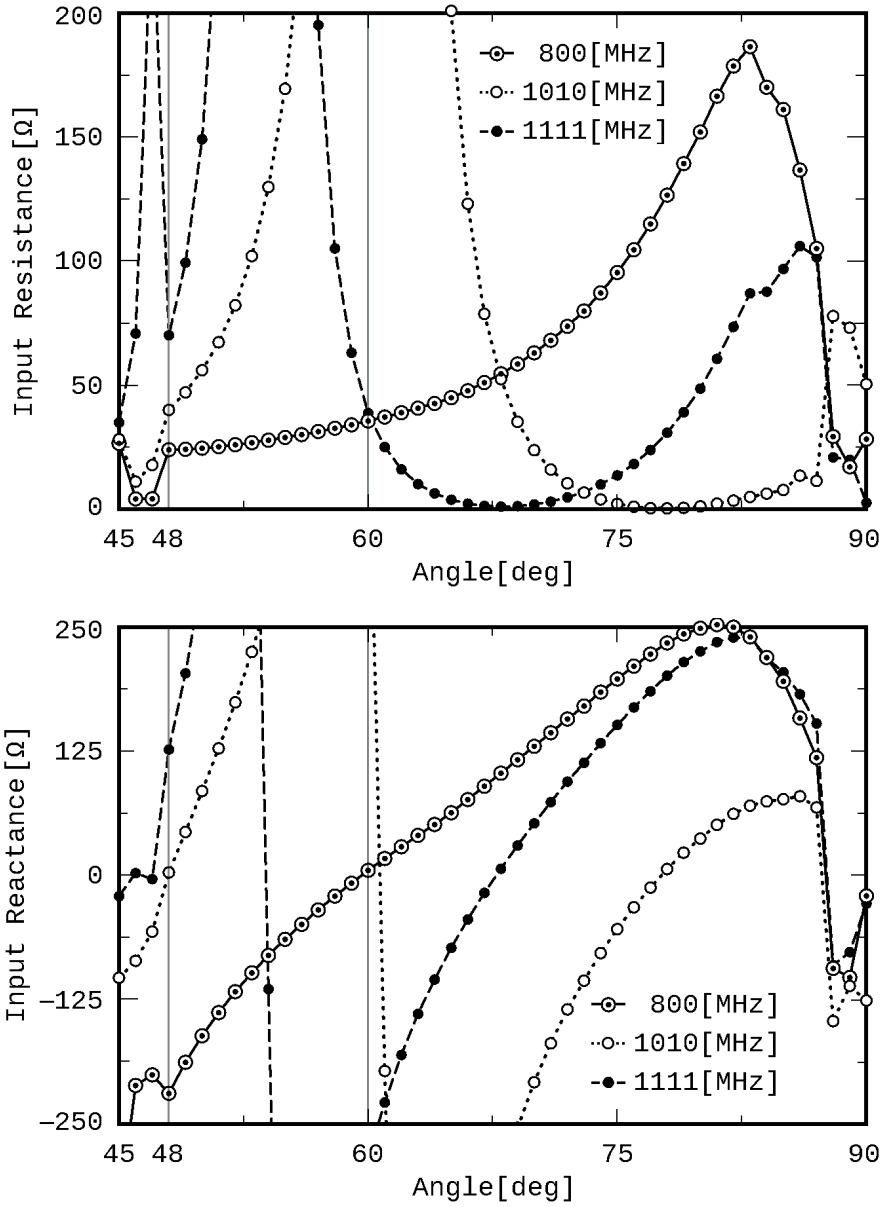

Fig 20: Input Impedance in a narrower range

References

[1] Papadaniel G.A., Yannopoulou N.I., Zimourtopoulos P.E., "A Planar Delta–Cross Shaped Loop Antenna: Analysis and Simulation – The 2 WL Case", FunkTechnikPlus # Journal, Issue 7, Year 2, February 2015, pp. 19-36
http://www.otoiser.org/index.php/ftpj/article/view/53
http://www.otoiser.org/index.php/ftpj/issue/view/2015.05.31

[2] Zimourtopoulos P., "Antenna Notes 1999-, Antenna Design Notes 2000-, http://www.antennas.gr/antennanotes/ (in Greek)

[3] Yannopoulou N., Zimourtopoulos P., "A FLOSS Tool for Antenna Radiation Patterns", Proceedings of 15th Conference on Microwave Techniques, COMITE 2010, Brno, Czech Republic, pp. 59-62

[4] Richmond J.H., "Computer program for thin-wire structures in a homogeneous conducting medium", Publication Year: 1974, NTRS-Report/Patent Number: NASA-CR-2399, ESL-2902-12, DocumentID: 19740020595, http://ntrs.nasa.gov/

[5] Yannopoulou N., Zimourtopoulos P., "Mini Suite of Antenna Tools, Educational Laboratories, Antennas Research Group, 2006, http://www.antennas.gr/antsoft/minisuiteoftools/

[6] Yannopoulou N.I., "Study of monopole antennas over a multi-frequency decoupling cylinder", PhD Thesis, EECE, DUTh, February 2008 (in Greek), pp. (2-6)-(2-9)

[7] Papadaniel G., "The Eisernes Kreuz Antenna [Prototype ARG-06]", Diploma Thesis #40, ARG–Antennas Research Group, DUTh, 2007 (in Greek)

*Active Links: 27.09.2015

Previous Publication in FUNKTECHNIKPLUS # JOURNAL

"A Planar Delta–Cross Shaped Loop Antenna: Analysis and Simulation – The 2 WL Case", Issue 7, Year 2, pp. 19-36

* About The Authors

Nikolitsa Yannopoulou, Issue 1, Year 1, p. 15

Petros Zimourtopoulos, Issue 1, Year 1, p. 15